Takayuki Tanji
抄読会 2023/8/25

Cancer-Associated Fibroblasts in Mycosis Fungoides Promote Tumor Cell Migration and Drug Resistance through CXCL12/CXCR4

Anna Aronovich, Lilach Moyal, Batia Gorovitz, et al. J Invest Dermatol. 2021 Mar;141(3):619-627.

がん細胞は正常線維芽細胞をがん関連線維芽細胞（CAF）に再プログラムし、腫瘍の支持体として働くことが知られている。皮膚 T 細胞リンパ腫の最も一般的なタイプである菌状息肉症（MF）における CAF の存在と役割は不明である。この研究では、早期 MF 患者と健常人のパンチ生検から得た初代線維芽細胞培養を用いて、MF における CAF の特徴とリンパ腫細胞とのクロストークを明らかにしようとした。

MF の培養では、CAF マーカーである FAP α と、CAF に関連する遺伝子とタンパク質である CXCL12（MF 細胞に発現する CXCR4 のリガンド）、コラーゲン XI、マトリックスメタロプロテアーゼ 2 のレベルが有意に増加した。培養 MF 線維芽細胞は、ex vivo 実験では正常線維芽細胞よりも大きな増殖を示した。MF 細胞株である MyLa 細胞との共培養は、正常線維芽細胞の増殖を増加させ、MyLa 細胞のドキソルビシンに対する感受性を低下させ、遊走を亢進させた。CXCL12/CXCR4 軸を阻害すると、MyLa 細胞のドキソルビシン誘導アポトーシスが増加し、MyLa 細胞の運動性が低下した。我々のデータは、MF 病変の線維芽細胞は正常皮膚の線維芽細胞よりも増殖性が高く、CAF は CXCL12 の分泌を介して MF 細胞をドキソルビシン誘導性の細胞死から保護し、遊走を増加させることを示唆した。MF における CAF が介在する腫瘍微小環境を逆転させることは、抗癌剤治療の効率を改善する可能性がある。

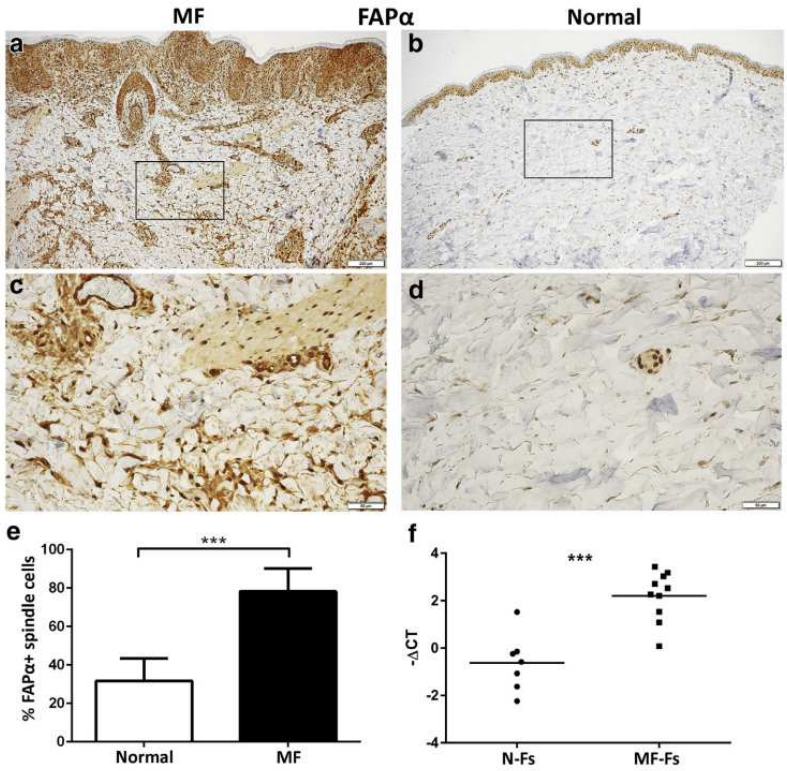

Figure 1. Identification of in situ and primary culture FAPα-positive CAFs in early MF. (**a**–**d**) Representative IHC images of FAPα staining showing a higher number of FAPα-positive spindle cells in the upper dermis of MF tissue than in normal skin. Bars = 200 mm and 50 mm. (**e**) Bar plot showing the mean (±SEM) percentage of FAPα-positive spindle cells in MF lesions (n = 10) compared with those in normal skin (n = 7). (**f**) Expression of *FAPα* gene in primary fibroblast cultures of MF-Fs compared with those of N-Fs on the basis of qRT-PCR. CAF, cancer-associated fibroblast; IHC, immunohistochemistry, MF, mycosis fungoides; MF-F, fibroblast from patient with MF; N-F, fibroblast from control subject; qRT-PCR, quantitative RT-PCR.

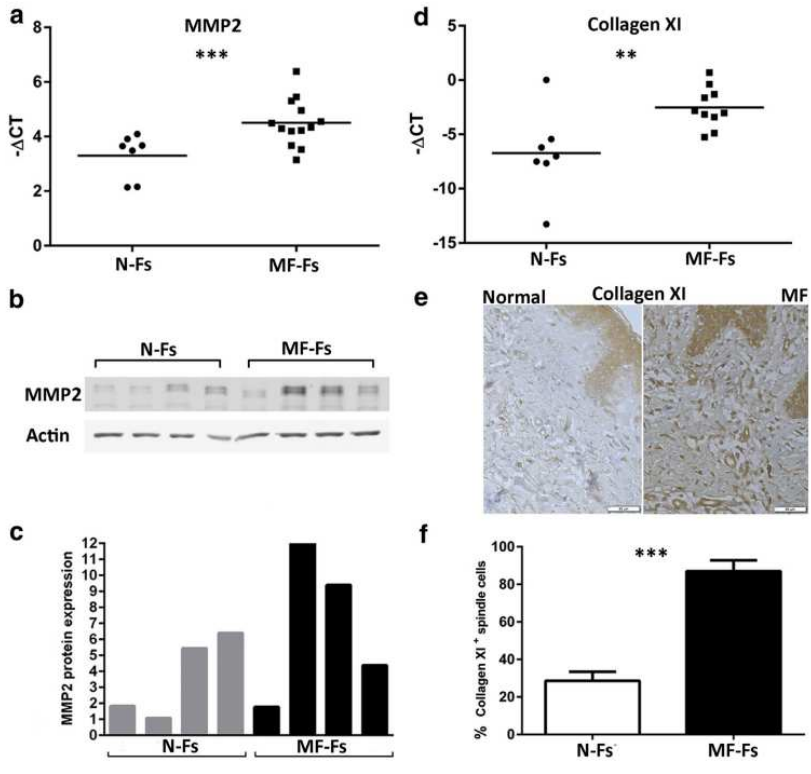

Figure 2. High expression of ECM remodeling genes and proteins in MF-CAFs. (**a**) High MMP2 gene expression in primary fibroblast cultures of MF-Fs (n = 12) versus those of N-Fs (n = 7), detected by qRT-PCR. (**b**) Representative western blots showing higher MMP2 protein expression in MF-F than in N-F cultures and densitometry quantification of MMP2 normalized to actin (n = 4 each). (**c**) The bar plot shows the mean (±SEM) percentage of MMP2 protein in cultures of MF-Fs compared with those of NF-Fs. (**d**) Higher collagen XI gene expression in primary fibroblast cultures of MF-Fs (n = 9) than in N-Fs (n = 7), detected by qRT-PCR. (**e**) Representative IHC images of intracellular pro-collagen XI staining showing a higher number of pro-collagen XI–positive spindle cells in the upper dermis of MF tissue compared with that of the normal skin. Bar = 50 mm. (**f**) The bar plot shows the mean (±SEM) percentage of pro-collagen XI–positive spindle cells in the upper dermis of MF lesions (n = 10) compared with that of the normal skin (n = 10). CAF, cancer-associated fibroblast; ECM, extracellular matrix; IHC, immunohistochemistry, MF, mycosis fungoides; MF-F, fibroblast from patient with MF; MMP2, matrix metalloproteinase 2; N-F, fibroblast from control subject; qRT-PCR, quantitative RT-PCR.

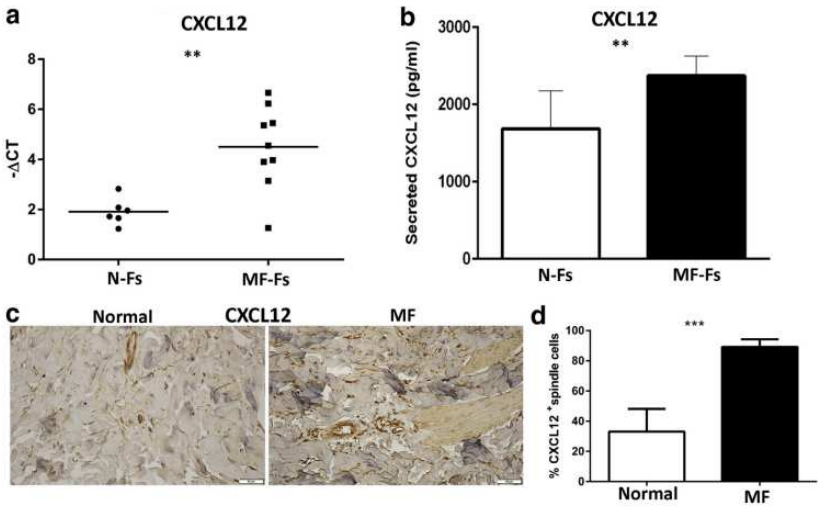

Figure 3. High expression of CXCL12 by MF-CAFs. (**a**) High CXCL12 expression in primary cultures of MF-Fs (n = 9) compared with those of N-Fs (n = 6), detected by qRT-PCR. (**b**) The bar plot shows a higher average extracellular CXCL12 concentration in the culture medium of MF-Fs than in that of N-Fs, detected by ELISA. (**c**) Representative IHC images of CXCL12 staining showing a higher number of CXCL12-positive spindle cells in the upper dermis of MF tissue than in normal skin. Bar = 50 mm (**d**) The bar plot shows the mean (±SEM) number of CXCL12-positive spindle cells in the upper dermis of MF tissue (n = 10) compared with that of normal skin (n = 10). CAF, cancer-associated fibroblast; IHC, immunohistochemistry, MF, mycosis fungoides; MF-F, fibroblast from patient with MF; N-F, fibroblast from control subject; qRT-PCR, quantitative RT-PCR.

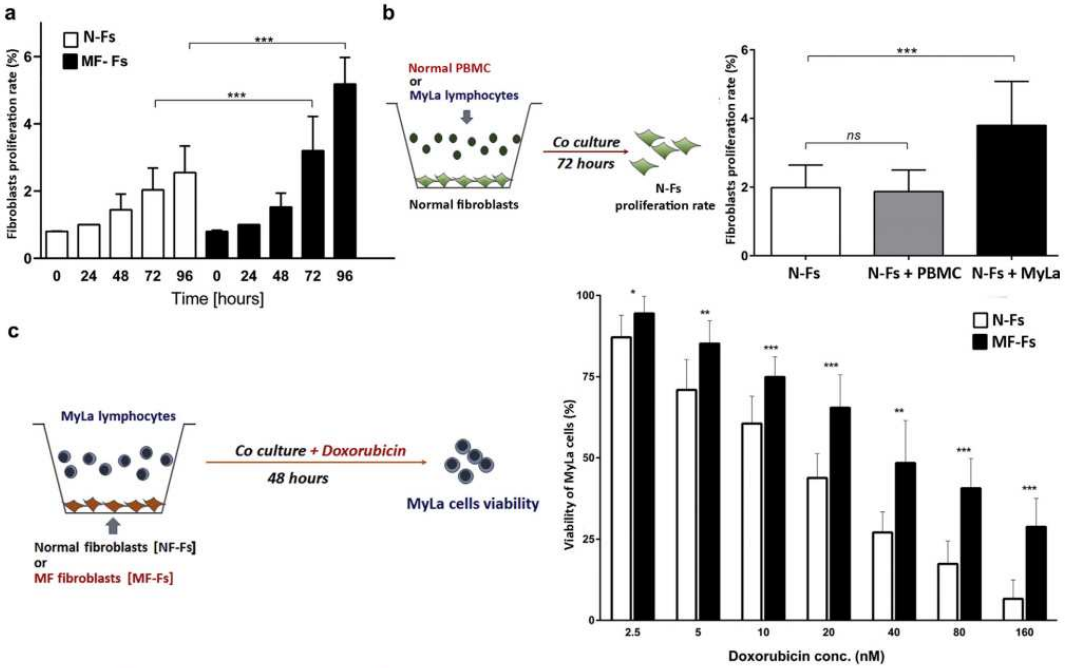

Figure 4. High proliferation of MF-CAFs and their contribution to MyLa chemoresistance. (**a**) Fold change of cell viability (XTT assay) is presented as proliferation rate. MF-Fs (n = 9) were more proliferative than N-Fs (n = 9). (**b**) Schematic chart of N-F proliferation in coculture. N-Fs were seeded and adhered at the bottom; floating PBMC or MyLa lymphocytes. The bar plot shows the mean (±SEM) proliferation rate after 72 hours (XTT): NF-Fs compared with N-Fs + normal lymphocytes and N-Fs + MyLa cells. (**c**) Schematic chart of MyLa survival in coculture with Doxo treatment. Fibroblasts were seeded and adhered at the bottom of the wells; N-Fs or MF-Fs and floating MyLa lymphocytes. The bar plot shows the mean (±SEM) number of MyLa cells collected at 48 hours after the addition of Doxo, 2.5–100 nM (XTT): N-F coculture (white column, n ≥ 6) compared with MF-F coculture (black column, n ≥ 6). CAF, cancer-associated fibroblast; conc., concentration; Doxo, doxorubicin; MF, mycosis fungoides; MF-F, fibroblast from patient with MF; N-F, fibroblast from control subject; ns, not significant; PBMC, peripheral blood mononuclear cell; XTT, Cell Proliferation Kit II.

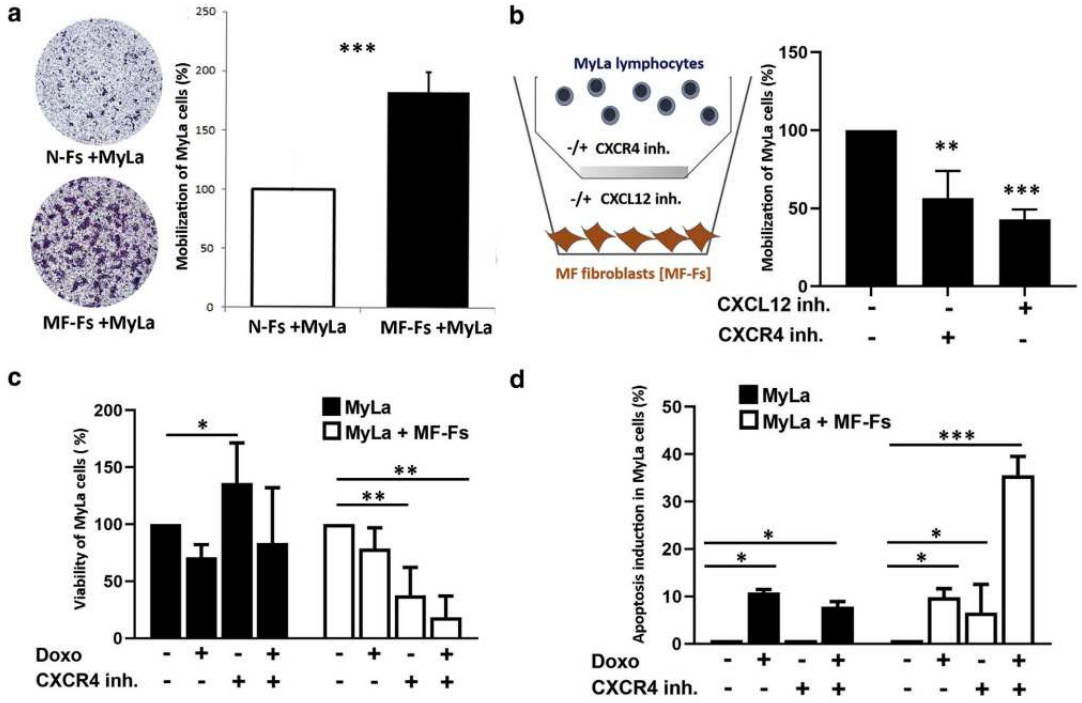

Figure 5. High MyLa cell proliferation and chemoresistance in coculture with MF-Fs, mediated by CXCL12/CXCR4 axis. (**a**) Mobilization of MyLa cells (crystal violet) in transwells of cocultured MF-Fs versus N-Fs by light microscopy (×10). The bar plot shows the mean (±SEM) percentage of migrated MyLa in coculture with MF-Fs or NF-Fs. (**b**) Schematic chart of MyLa cell mobilization in coculture with MF-Fs under treatment with CXCL12 and CXCR4 inhibitors. The bar plot shows the mean (±SEM) number of untreated MyLa cells (represented as 100%) versus treated MyLa cells ($n \geq 10$). (**c**) Bar plots showing MyLa cell viability by XTT and apoptosis by flow cytometry with (**d**) Annexin and/or PI staining after 48-hour culture alone or with MF-Fs under treatment with Doxo (20 nM), CXCR4 inh., or both. inh., inhibitor; Doxo, doxorubicin; MF, mycosis fungoides; MF-F, fibroblast from patient with MF; N-F, fibroblast from control subject; PI, propidium iodide; XTT, Cell Proliferation Kit II.

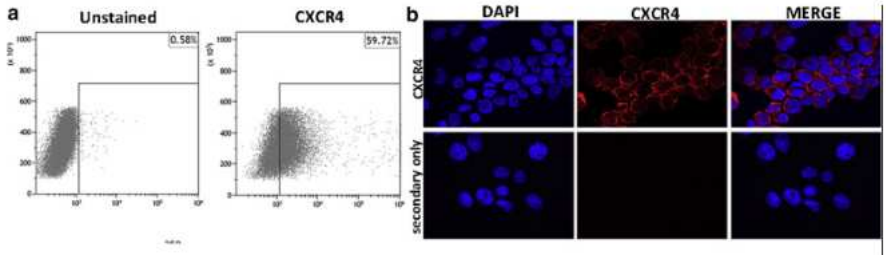

Supplementary Figure. **CXCR4 expression on MyLa cells.**
(**a**) Representative flow cytometry graph showing CXCR4 staining on MyLa cells. (**b**) Immunofluorescence of membranal CXCR4 in MyLa cells.

●Take home message

MF 培養において CAF マーカーである FAPα と、CAF に関連する遺伝子とタンパク質である CXCL12（MF 細胞に発現する CXCR4 のリガンド)、コラーゲン XI、マトリックスメタロプロテアーゼ 2 のレベルが有意に増加した。

標準的な単化学療法と組み合わせて MMP2 を阻害するか、またはコラーゲン XI 代謝回転を低下させることが、MF 治療の効率を改善するための有望なアプローチである可能性がある。

MyLa 細胞由来の CXCR4 の阻害剤はドキソルビシンと相乗的にアポトーシスを誘導することにより、MF-Fs 細胞存在下で MyLa 細胞の生存率を低下させる可能性がある。